INTERNATIONAL JOURNAL OF CLIMATOLOGY
Int. J. Climatol. **24**: 1283–1306 (2004)
Published online in Wiley InterScience (www.interscience.wiley.com). DOI: 10.1002/joc.1058

REGEOTOP: NEW CLIMATIC DATA FIELDS FOR EAST ASIA BASED ON LOCALIZED RELIEF INFORMATION AND GEOSTATISTICAL METHODS

AXEL THOMAS[a,*] and UTE C. HERZFELD[b]
[a] *Geographisches Institut, Johannes-Gutenberg Universität, 55099 Mainz, Germany*
[b] *National Snow and Ice Data Center, Cooperative Institute for Research in Environmental Sciences, University of Colorado Boulder, Boulder, CO 80309-0449, USA*

Received 21 July 2003
Revised 7 April 2004
Accepted 20 April 2004

ABSTRACT

Climate data fields represent essential tools for climate, biogeographical and agricultural research to run models and to provide observational data for the verification of global climate models (GCM). Climate data fields are generated through interpolation of observations taken at meteorological stations. Most current interpolation procedures try to describe the influence of topography on spatial climatic variations by relating them directly to absolute elevation or by introducing simple relief variables such as exposure. In both cases this may not properly describe spatial climatic variations, particularly not those of precipitation.

This paper describes a regionalization procedure (REGEOTOP) that was applied to generate monthly spatial climatic data fields of temperature, precipitation and potential evapotranspiration (1951–90) for East Asia at 0.25° resolution from a new climate data base. REGEOTOP proceeds in several steps, combining statistical and geostatistical methods. First, basic relief types are determined by application of principal component analysis to moving windows in a digital elevation model (DEM) of the study area. Second, climatic variables are related to relief parameters by regression analysis with respect to basic relief types, location, and elevation. To account for large-scale variation of climate variables, geostatistical variogram analysis (step three) and interpolation (step four) are applied to the regression residuals. Finally, maps of regression estimates plus kriged residuals are calculated, for a total of 1440 cases.

The relief parameterization retains about 90% of the variance of a DEM in 10–18 principal components, depending on input parameters. The REGEOTOP method is computationally expensive, but results justify the effort. Owing to the thorough analysis in the REGEOTOP method and its application to the most comprehensive climate databases that exist outside China to date, the resultant maps provide a solid basis for GCM verification or hydrological and agro-ecologic investigations and prognoses for East Asia. Copyright © 2004 Royal Meteorological Society.

KEY WORDS: East Asia; regionalization; geostatistics; data fields; topography; precipitation; temperature; evapotranspiration

1. INTRODUCTION

Despite intensive research for several decades (WMO, 1972) the interpolation of climatic data, particularly in mountainous regions, to obtain spatially distributed data sets has remained a problem. Even if multivariate or geostatistical interpolation methods are applied (e.g. Hutchinson, 1995a; Martinez-Cob, 1996), direct interpolation without inclusion of topographic data cannot capture the spatial climatic variability unless an unrealistically high station density is available. Including elevation information from a digital elevation model (DEM) in the regionalization procedure (e.g. Phillips *et al*., 1992; Hudson and Wackernagel, 1994; Hutchinson, 1995b; Fleming *et al*., 2000; Goovaerts, 2000; New *et al*., 2002) will only lead to improved results if elevation is actually describing the spatial variation of the climatic element within the study area.

* Correspondence to: Axel Thomas, Geographisches Institut, Johannes-Gutenberg Universität, 55099 Mainz, Germany; e-mail: a.thomas@geo.uni-mainz.de

In most cases, climatologically relevant processes, such as orographic lifting of air masses, are influenced by morphological aspects and relative elevation differences of the local topography rather than by absolute altitude alone.

To account for the influence of the topography variables, such as exposure, slope or distance and elevation difference to the highest topographic barrier have been used (see Prudhomme and Reed (1998)), in particular in the regionalization of precipitation data. Ever since early attempts to employ topographic variables in the late 1940s by Spreen (1947), topographic variables have almost exclusively been designed based on the individual scientist's assumption of which topographic variables contribute particularly to the explanation of the spatial behaviour of the climate element in question. As such, they have to be regarded as subjective as other, more important variables may have been overlooked and may not have been included in the analysis.

This paper describes the application of an objective method for the determination of topographic variables based on principal component analysis (PCA) of a DEM. Stepwise multivariate regression, geostatistical analysis and interpolation ('kriging') are then used to calculate monthly climate maps. In view of the importance placed by the scientific community on spatial climate data of China (Baker, 1999), temperature, precipitation and evapotranspiration maps have been derived for East Asia with particular emphasis on China.

2. STUDY AREA AND DATA

The study area includes the land area of the People's Republic of China (including Tibet) and adjacent areas of East, South and Central Asia (Figure 1). The area represents about one-tenth of the global land area with elevations ranging from −156 m (Turpan Basin) to 8848 m (Mt Everest). The topography of that region is organized in three more or less concentric levels (Ren, 1985), with the lowest southern and eastern part consisting of coastal plains and rolling hill country below 1500 m, the intermediate level of basins and mountain ranges between 1500 and 3000 m, and the highest level with the Tibetan Plateau and high mountain ranges, such as the Himalayas, above 3000 m. Summer precipitation south of approximately 35 °N is mainly derived from southeast and southwest monsoonal air masses and from extratropical westerlies to the north. In terms of annual precipitation, some of the wettest (>3500 mm/year, Taiwan northeast coast) and driest (northern Taklimakan Desert, <20 mm/year) places in East Asia can be found within the study area. Similarly, annual potential evapotranspiration (PET) values vary from <550 mm (Sichuan Basin) to >2800 mm (eastern Taklimakan Desert), and mean annual temperatures range from 24 °C along the South China coast to −5 °C on the Tibetan Plateau.

Time series data were available for 531, 672 and 196 stations for temperature, precipitation and PET respectively, with the majority of the data covering the period from 1951 to 1990 (Figure 2). With few exceptions, meteorological stations are maintained by the Chinese Bureau of Meteorology and are operated according to international standards. PET was estimated using the Penman–Monteith method (Allen *et al*., 1998) using ET V1.0 software from Cranfield University (Hess and Stephens, 1993). The major part of the

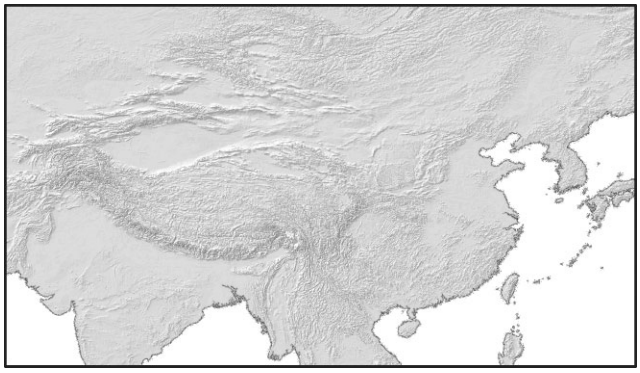

Figure 1. DEM (GTOPO30) of the study area

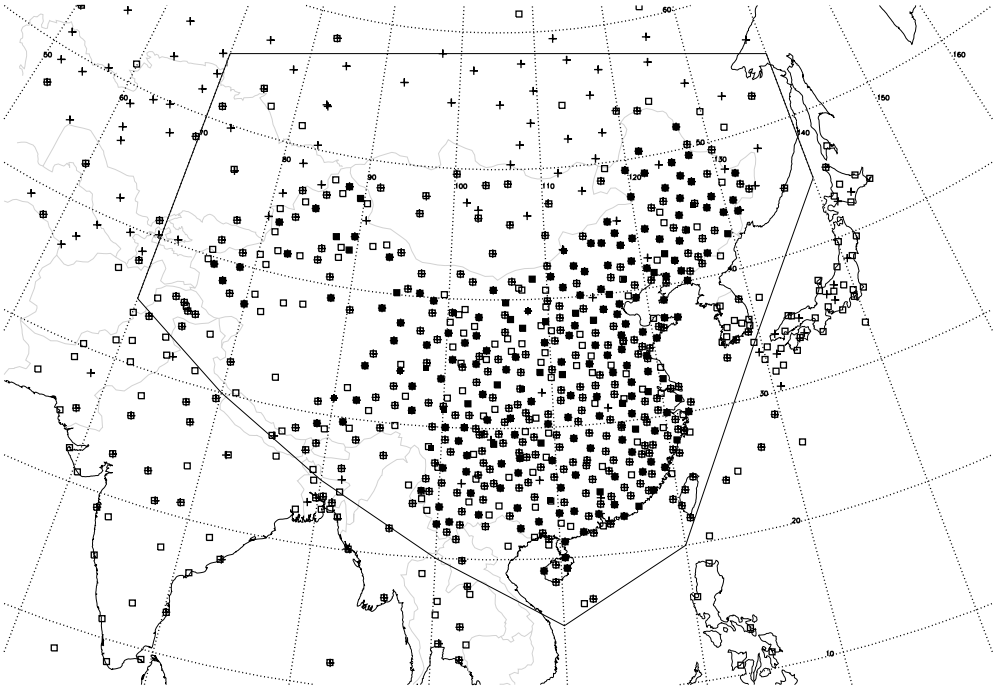

Figure 2. Station distribution in the study domain. Open squares denote temperature stations, filled squares are precipitation stations and crosses are stations with estimated PET data. The polygon outlines the model area

time series was collected during field work in China with additional data added from the Carbon Dioxide Information Analysis Center (CDIAC; Tao *et al*., 1991; Kaiser *et al*., 1993) and the Global Historical Climate Network (GHCN, Version 2; Peterson and Vose, 1997). Selected high-altitude station data in Central Asia are by courtesy of H. Böhner, Göttingen University, Germany. Only time series that passed the Mitchell (1966), Buishand (1982) and Abbe (Schönwiese and Malcher, 1985) checks for homogeneity were included in the analysis. Elevation data were taken from GTOPO30, a DEM with global coverage at 30″ resolution (approximately 1 km) supplied by the US Geological Survey (USGS, 2000). DEM data were clipped to the spatial extent visible in Figure 1.

3. REGIONALIZATION METHODOLOGY FOR CLIMATIC DATA INCLUDING RELIEF INFORMATION

Parameterization of the topography as input to climate regionalization procedures has mainly been in the form of variables that are considered to reflect properties of the topography that influence climate. Variables commonly employed are average elevation, slope angle and aspect, elevation difference between station and neighbouring ranges, number of repeated occurrences of mountain chains and distance to the coastline (e.g. Scherer, 1977; Hughes, 1982; Parker, 1982; Hormann, 1985; Basist *et al*., 1994; Leblois and Desurosne, 1994; Hutchinson, 1995b; Konrad, 1996; Hay *et al*., 1998; Prudhomme and Reed, 1998). In most cases the variables have been calculated for several aspect and/or distance classes. A different approach was taken by Daly *et al*. (1997), who evaluated the statistical distribution of slope conditions in rectangular windows.

A multivariate stepwise regression with the topographic variables as independent predictors and the observed climate value as dependent variable is commonly applied to sort the topographic variables according to their explained variance. Deriving the topographic variables for each point in the whole study area and inserting them into the regression equation yields a climate field prediction. This approach assumes that the study area is either climatically homogenous or small enough so that the influence of effects not related to topography

remains constant within the study area. Large-scale gradients, such as the influence of changing latitude or longitude, are either neglected or accounted for by including longitude and latitude in the input variables (Schermerhorn, 1967; Hormann, 1985; Hudson and Wackernagel, 1994; Hutchinson, 1995b). This approach has the advantage that it may be customized to reflect any climate characteristics specific to the study area; however, important features of the topography relevant for the spatial properties of the climatic element may be lost.

In order to provide a more objective method to account for the influence of topography, Benichou and Lebreton (1987) have proposed to parameterize topography with the help of a PCA. For each element of the DEM a relative topography is obtained by subtracting its elevation from the elevation values of a square window (e.g. 5×5 or 11×11 elements) centred on that element. In the statistical context, each element of the window is seen as a variable and each DEM element is seen as a case or object. After rearranging the results of each window as input data for the PCA, each row of the input matrix represents one case and each column represents one variable (Figure 3).

The input matrix is subjected to an R-mode PCA (Richman, 1986). The relative topography in the domain can then be described as a linear combination of the resulting eigenvectors of the minor product of the input matrix weighted by their corresponding principal components (PCs). Each eigenvector is interpreted as a 'base topography' ('paysage du base'; Benichou and Lebreton, 1987) representing different basic morphological elements, such as domes or depressions, slopes, saddles or parallel ridges of different exposition or different orientation. With decreasing variance, PCs explain increasingly complex topographic features that defy easy descriptions. This approach allows the topography around a station to be decomposed into the PCs of its relative landscape and the absolute altitude of the station itself. As PCs are not correlated with each other, they offer an added advantage as predictors for a regression analysis.

Stepwise multiple linear regression is then used to select significant predictors for the observed climatic values (such as a monthly or annual mean value) from relative topographies decomposed into base topographic components (PCs) and absolute altitude. Application of the regression equation to each element of the DEM then results in a predicted climate data field. The residuals between observed and predicted values

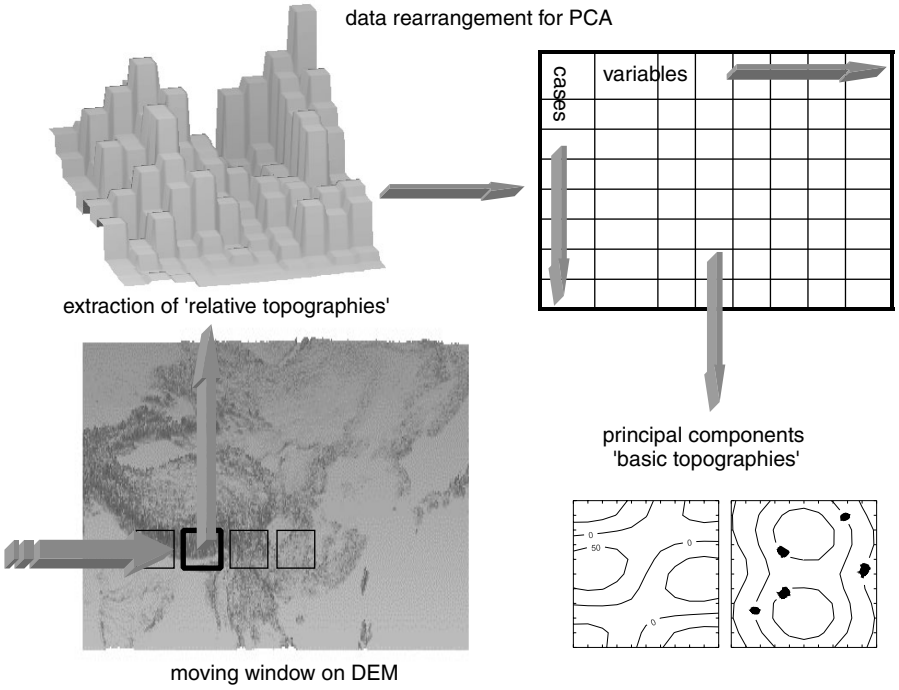

Figure 3. Schematic view of extraction of localized relief information from the DEM and rearrangement of extracted data for PCA

are interpolated via a geostatistical method (kriging) and added to the regression field to account for any remaining spatial variation. Peck and Brown (1962) initially introduced the idea to add an interpolated field of residuals to the results of a functional relationship between climatic processes and topography to account better for both topography-related processes and any other remaining influences. The regionalization method has been termed 'AURELHY' ('Analysis Using the Relief for Hydrometeorology'; Benichou and Lebreton, 1987) and has been adopted by the French Weather Service (Météo France) as the standard for the preparation of climate maps.

Similar procedures that include a first step of detrending and a second step of kriging have been applied in climatological data analysis and termed 'modified residual kriging' (Martinez-Cob, 1996; Prudhomme and Reed, 1999) or 'detrended kriging' (Holdaway, 1996) or 'kriging with a guess field' (Ahmed and De Marsily, 1987).

4. REGEOTOP: ADAPTATION OF THE AURELHY METHOD FOR CONTINENT-SIZED AREAS

The AURELHY method assumes that topography-related influences are the major variables describing the spatial organization of climate within a study area. When the method is applied to a large region, such as East Asia, continent-scale effects such as the latitudinal decrease of temperature or the influence of different monsoon air masses (Domrös and Peng, 1986) have to be accounted for. Segmenting the study area in smaller, climatically homogeneous regions is not feasible due to the low station density in some of the individual regions, which would result in samples too small for statistically significant regression solutions. Instead, latitude and longitude have been added as additional predictors in the regression equation. The actual model area was restricted to the polygonal area shown in Figure 2. Integrating stations outside of this area into the regression equations resulted in dramatically decreased correlation coefficients. This indicates different responses of climatic variables to topographic forcing inside and outside of the model area that are thought to be related to different airflow directions in the main circulation features involved, namely the East Asian and the South Asian monsoon systems. Outside of the model area, geostatistical interpolation alone was used to calculate grid values.

Our approach has been termed REGEOTOP (Regionalization with Geostatistics and Topography) and improves the original concept, as it extends the applicability to larger areas than the original. The computational steps of REGEOTOP are summarized in the Appendix. The advantages of REGEOTOP are:

1. Objective analysis of the local relief using PCA allows us to take the complex relief of China into account; this is a vast improvement over the utilization of a small number of relief parameters.
2. Both large-scale (continental-scale) and local topographic influences are integrated into the regionalization procedure.
3. The same relief analysis may be used for mapping all three climate variables, i.e. temperature, precipitation and PET.

REGEOTOP is computationally expensive relative to the capacity of a personal computer, but the results justify this effort. The algorithm of our method has been programmed using IDL.

4.1. Theoretical considerations

We consider a decomposition of the climate variable V_α into a location, elevation and relief component f, and a residual ε, as follows:

$$V_\alpha\ (x, y, z, R) = f_\alpha\ (x, y, z, R) + \varepsilon_\alpha\ (x, y, z, R) \tag{1}$$

where α is an index for the climate variable ($\alpha = 1$, temperature; $\alpha = 2$, precipitation; $\alpha = 3$, PET), x, y coordinates (x, longitude; y, latitude), z elevation, with (x, y, z) in a domain D in $\mathcal{R}^3$ and R relief information.

Information on the variable model V_α is given in terms of climate observations at (discrete) stations:

$$V_\alpha(P_i) = V_\alpha(x_i, y_i, z_i, R_i) = f_\alpha(x_i, y_i, z_i, R_i) + \varepsilon_\alpha(x_i, y_i, z_i, R_i) \tag{2}$$

where P_i is observation point ($i \in J$, J an index set), x_i, y_i, z_i longitude and latitude coordinates and elevation, and R_i is the local relief information in the neighbourhood of point P_i.

The relief information R_i is obtained by localized PCA, carried out for the DEM of East Asia. R is a symbolic 'variable', indicating the following procedure:

$$z = z(x, y) \text{ is elevation in location } (x, y) \tag{3}$$

Elevation is decomposed into a regional component z_r and a global component z_g:

$$z = z(x, y) = z_\mathrm{g}(x, y) + z_\mathrm{r}(x, y) \tag{4}$$

For a window of size $W \times W$ and a location (x, y), the regional elevation component z_r is obtained by calculating differences of elevation values inside the window:

$$z_\mathrm{r}(x_{i-j}, y_{i-t}) = z(x_{i-j}, y_{i-t}) - z(x_i, y_i) \tag{5}$$

All z_r values are rearranged into a matrix with each row containing consecutive z_r values of a single window.

Then, a PCA of z_r is done. The R values are the base topographies which are the PCs $\mathrm{PC}_1, \ldots, \mathrm{PC}_k$, in the PCA. In practice, the regression is carried out for each variable and month and year:

$V_{\alpha,\beta,\gamma}$ $\alpha \in \{\text{temperature, precipitation, PET}\}$, $\alpha = 1$, temperature, $\alpha = 2$, precipitation, $\alpha = 3$, PET

$\beta \in \{1, 2, \ldots, 12\}$, 1 = January, 2 = February, ..., 12 = December

$\gamma \in \{1951, \ldots, 1990\}$, year

The regression equation then reads

$$V_{\alpha,\beta,\gamma} = a_1 x + a_2 y + a_3 z + a_4 \mathrm{PC}_1 + \cdots + a_{(3+k)} \mathrm{PC}_k \tag{6}$$

and is carried out for

$$V_{\alpha,\beta,\gamma}(P_i) = a_1 x_i + a_2 y_i + a_3 z_i + a_4 \mathrm{PC}_1(i) + \cdots + a_{(3+k)} \mathrm{PC}_k(i) \tag{7}$$

with $i = 1, \ldots, n$ stations P_i, (x_i, y_i, z_i) station coordinates and elevation, and $a_1, \ldots, a_{3+k}$ are the regression coefficients. To obtain R_i (relief decomposition), in the DEM raster of East Asia, the raster element containing the station P_i is identified, and the relief decomposition of this element is used. We call it R_i (with the same index, for simplicity). It has base topographies $\mathrm{PC}_1(i), \ldots, \mathrm{PC}_k(i)$, k is as in Table I (e.g. $k = 18$).

For each (α, β, γ), a regression analysis with z dependent on the base topographies is carried out, then the residual $\varepsilon_{\alpha,\beta,\gamma}(x, y, z, R)$ is obtained. In the geostatistical part, variography and ordinary kriging will be applied to $\varepsilon_{\alpha,\beta,\gamma}(x, y)$ in $\mathcal{R}^2$.

4.2. Practical considerations

The information that is retained in the principal components of the relief parameterization depends both on the resolution R of the input DEM and of the size of the moving window, quantified here by the parameter W for a rectangular window of the size $W \times W$ grid nodes. Decreasing R while keeping W constant covers a larger area but analyses a smoothed topography, thereby losing information on small-scale topographic

Table I. PCA results for several combinations of R and W[a]

R	W	PC_1	PC_2	PC_3	PC_4	PC_5	PC_6	PC_7	PC_8	PC_9	PC_{10}	PC_{11}	PC_{12}	PC_{13}	PC_{14}	PC_{15}	PC_{16}	PC_{17}	PC_{18}	PC_{19}	PC_{20}	A	B	C
1200″	5	**37.2**	**28.8**	**9.1**	**3.7**	**3.4**	**2.2**	**1.9**	**1.5**	**1.2**	**1.2**	1.1	1.0	0.8	0.8	0.8	0.7	0.6	0.6	0.6	0.6	10	12	90.4%
1200″	11	**36.7**	**28.8**	**8.3**	**3.6**	**2.9**	**2.2**	**1.7**	**1.2**	**0.9**	**0.8**	**0.7**	**0.6**	**0.5**	**0.5**	**0.4**	**0.4**	0.4	0.3	0.3	0.3	16	8	85.4%
600″	5	**36.9**	**28.8**	**9.5**	**3.7**	**3.4**	**2.1**	**1.9**	**1.7**	**1.4**	**1.2**	1.0	1.0	0.8	0.8	0.8	0.7	0.7	0.6	0.6	0.6	10	12	90.4%
600″	11	**36.5**	**29.4**	**8.2**	**3.3**	**3.0**	**2.1**	**1.5**	**1.2**	**0.9**	**0.8**	**0.7**	**0.5**	**0.5**	**0.5**	**0.5**	**0.4**	**0.4**	0.3	0.3	0.3	17	8	85.2%
300″	5	**42.0**	**18.8**	**8.1**	**3.7**	**3.5**	**2.2**	**2.1**	**2.1**	**1.8**	**1.5**	**1.4**	**1.4**	**1.2**	**1.2**	1.1	1.1	1.0	1.0	0.9	0.9	14	18	91.0%
300″	11	**39.2**	**21.9**	**6.9**	**3.2**	**2.6**	**1.7**	**1.4**	**1.3**	**1.0**	**0.8**	**0.7**	**0.6**	**0.6**	**0.6**	**0.5**	**0.5**	**0.5**	**0.4**	0.4	0.4	18	9	78.3%
150″	5	**41.8**	**17.6**	**10.0**	**4.3**	**3.5**	**2.3**	**2.3**	**2.0**	**1.9**	**1.4**	**1.3**	**1.3**	**1.1**	1.0	1.0	1.0	0.9	0.8	0.8	0.8	13	16	90.8%

[a] R and W denote DEM resolution and window size respectively. PC variances marked in bold explain at least 90% of variance for the given combination of R and W. Column A gives the number of PCs with cumulative variances ≥90%, column B the number of PCs with individual variances ≥1% and column C the cumulative variance for PCs with individual variances ≥1%.

features. Keeping R high and increasing W to counteract this effect leads to large data matrices that are difficult to handle: a combination of $R = 300''$ and $W = 11$ results in more than 47 million elements.

Topographic features can assert a considerable influence on precipitation, even at large distances, as the condensation level of an air mass is shifted in ever increasing altitudes by the repeated crossing of mountain ranges (Fliri, 1967). On the other hand, several authors (Scherer, 1977; Benichou and Lebreton, 1987; Konrad, 1996; Prudhomme and Reed, 1998) have noted that correlations between topography and precipitation begin to decrease at DEM resolutions of less than 5 to 10 km (approximately 150 to 300″). To evaluate the effects of different combinations of R and W, four DEMs at resolutions of 150″, 300″, 600″ and 1200″ calculated from the original GTOPO30 were tested with window sizes from 5 to 11 pixels.

As a result of the PCA (see Table I), 10 to 18 PCs are needed to account for more than 90% of the variance of the whole DEM, depending on the selected values for R and W. With increasing DEM resolution, more PCs are needed to explain the finer topographic detail that can be resolved at higher resolutions when a larger window size is selected. If PCs are omitted that contribute only marginally ($<1\%$) to the total variance, then 78 to 91% of the DEM can be explained by 12 to 18 PCs.

In order to visualize the resulting base topographies, the eigenvectors are arranged according to the original location of the variables in the window (Figure 4). Mapping the PC scores demonstrates the relative contribution of the individual base topographies to the topography of the study area (Figure 5). The first PC, PC_1, identifies the locations of isolated mountain massifs or depressions with such prominent examples as Mt Everest or Daulaghiri. The second PC (PC_2) and the third (PC_3) describe exposition by marking linear structures that trend north–south or east–west respectively. The fourth principal component (PC_4) represents a complex structure consisting of parallel ridges and depressions at a 110° angle and identifies features that are related to prominent geological structures that occur especially in the central mountain ranges of eastern China. Different combinations of R and W display different levels of detail but have a similar spatial distribution of base topographies.

As the range of influence of the topography on the regional climate is unknown, trial runs with different combinations of R and W for different months were conducted for all three climate elements. Variation of selected predictors, their regression coefficients and explained variances were high, which indicates that the method easily detects the variable influence of the changing seasonal and interannual characteristics of the air masses in response to topographical forcing. No combination of R and W, however, resulted in a clearly superior result. Despite its relatively low ranking in terms of explained DEM variance, a combination of $R = 300''$ and $W = 11$ was selected as it gives a high spatial resolution without being computationally too expensive. At this DEM resolution the actual size of a moving window with $W = 11$ corresponds to approximately 300 km, similar to half ranges of precipitation coherence as given by Böhner (1996) for East and Central Asia.

To assess the temporal variation in detail the regression described above was applied to monthly temperature, precipitation and PET data for each year in 1951 to 1990 (a total of 1440 data sets; 12 months × 40 years × 3 climate elements). Hence, analysis of the spatial variability and kriging is preferred for each of the 1440 data sets also.

5. GEOSTATISTICAL EVALUATION AND MAPPING OF RESIDUALS

Geostatistics is applied here to the residuals of the regression, obtained as described in Section 4. Residuals may show large values, as some of the regional gradients do not always follow a linear relationship as assumed when applying a linear regression. Precipitation gradients in the mountains of southwest China have been shown to exhibit up to three maxima at different altitudes (Thomas, 1997). The high spatial variability of the residuals necessitates an interpolation; we utilize ordinary kriging here. The kriging method is explained in Herzfeld (1992).

Variography and ordinary kriging are applied to $\varepsilon_{\alpha,\beta,\gamma}\ (x,\ y)$ in $\mathcal{R}^2$. The residual $\varepsilon_{\alpha,\beta,\gamma}\ (x,\ y)$ is also a regionalized variable. In kriging, the following two steps are carried out:

1. Analysis of spatial structure of the variable (variography).

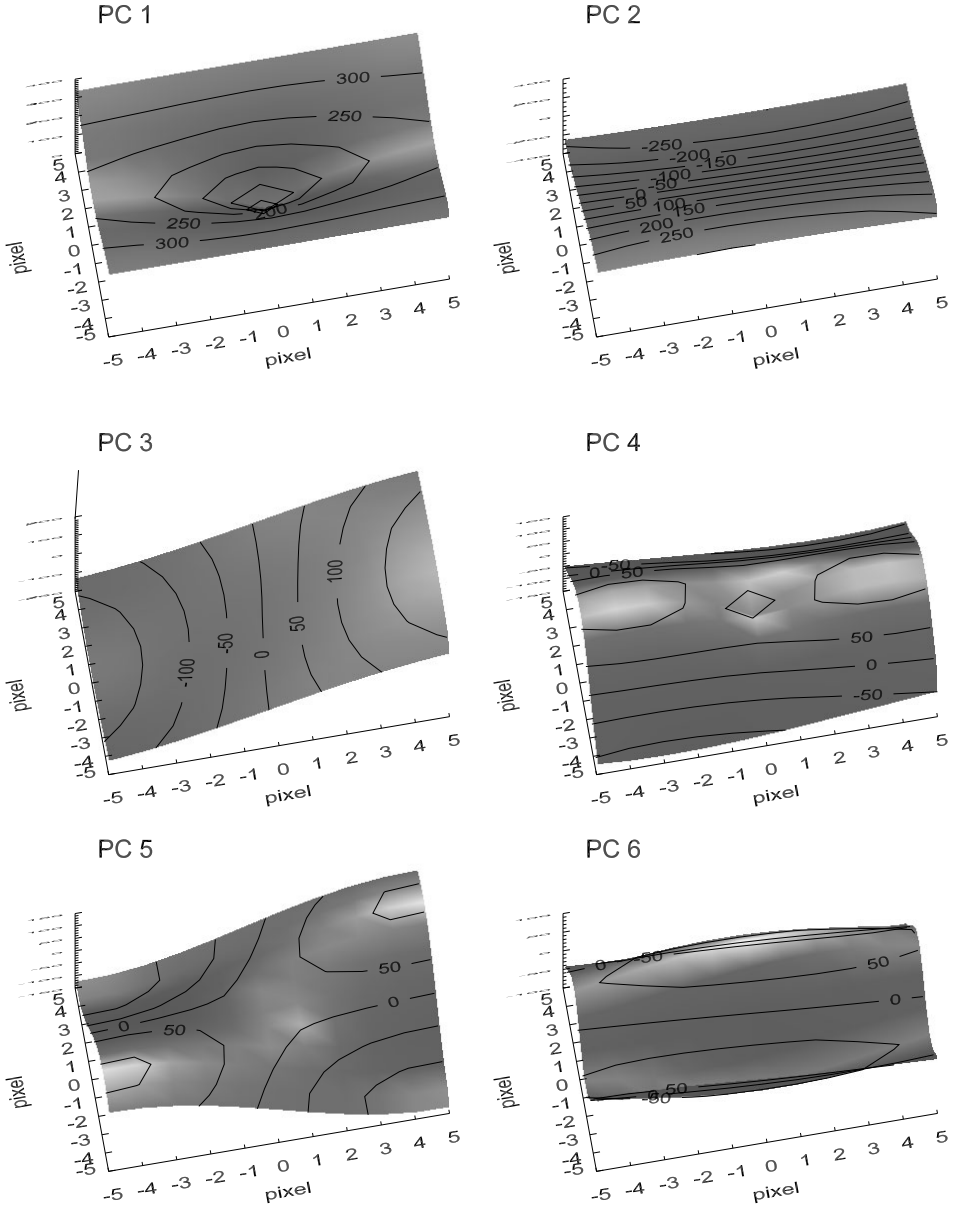

Figure 4. Three-dimensional illustration of base topographies (PCs) 1–6. Base topographies were calculated with a DEM of 300″ resolution and a window size of 11 pixels. These six base topographies explain about 76% of the DEM variance

2. Estimation of the variable, using results from the variography.

In our application, the variable is the residual $\varepsilon = \varepsilon_{\alpha,\beta,\gamma}$, which depends on (x, y, z) and the relief-parameterization R:

$$\varepsilon_{\alpha,\beta,\gamma} = \varepsilon_{\alpha,\beta,\gamma}(x, y, z, R) \tag{8}$$

Program UNIKRG (Herzfeld, 1990) is used in the estimation; program VARIO3D is used in variogram calculation and analysis.

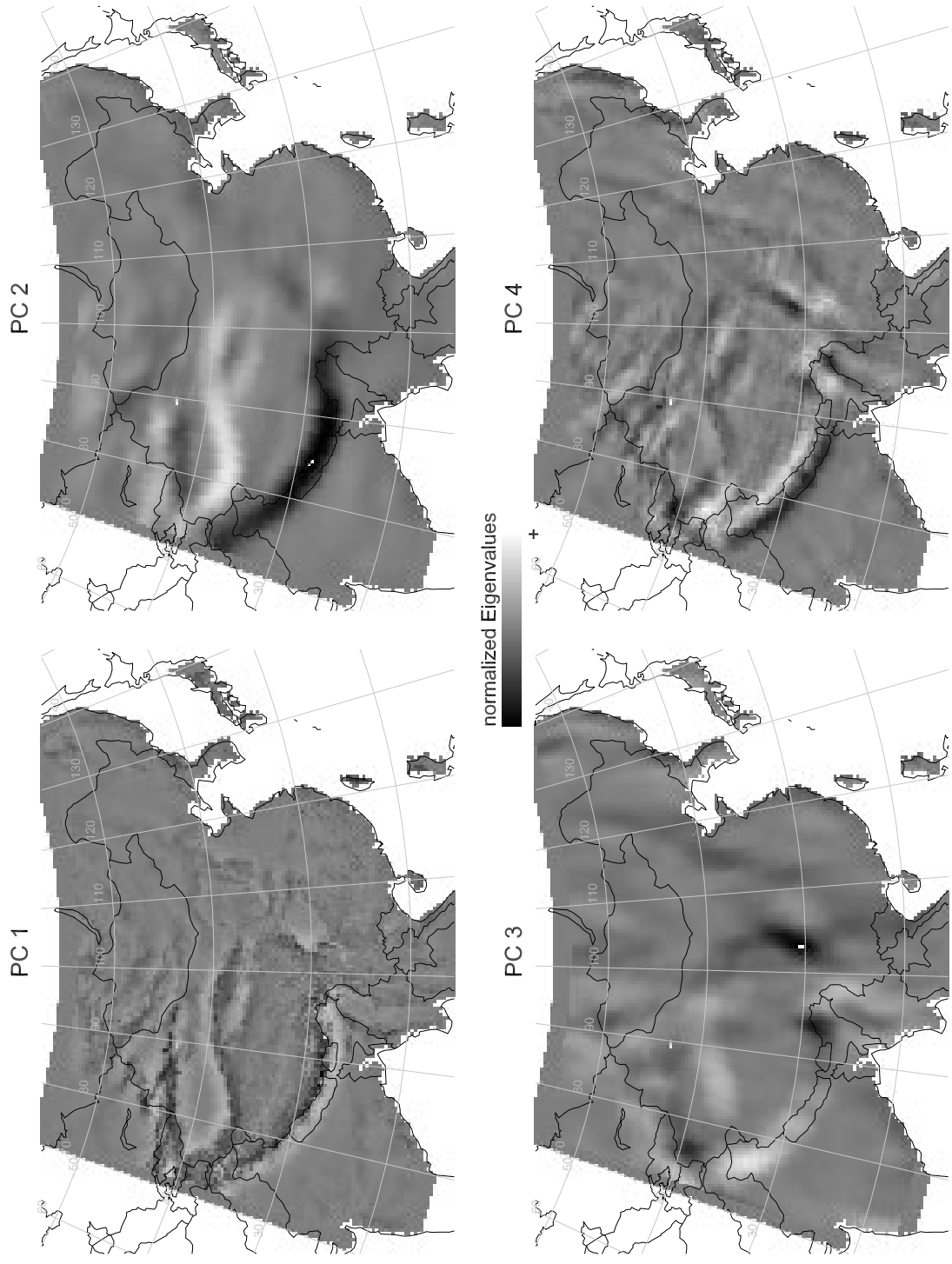

Figure 5. Spatial distributions of base topographies 1–4 in the study area. For base topography 1 (upper left) the darker shades indicate convex forms (summits) and the lighter shades are concave forms (depressions). DEM of 1200″ resolution, window size 11 pixels

For geostatistical interpolation using ordinary kriging, the experimental variogram is fitted by a variogram model, which needs to satisfy certain mathematical conditions to assure that the system of linear equations needed by the ordinary kriging system has a unique solution. Spherical and Gaussian models have proven both mathematically correct and practical.

For each of the 1440 cases, variograms were fitted by hand. Fitting of model parameters 'by hand' is more robust than an automated process (see Chilès and Delfiner (1999)). Here, fitting by hand (following the same objective procedure for each variogram) was necessary because of the high monthly and interannual variability of the variograms. Examples of the 1440 variograms are given in Figures 6, 8 and 9.

The dependence of the climate variables on topography is not isotropic; this may suggest the exploration of directional variograms. A study of directional variograms of the residuals however, indicated, that variograms did not show any larger anisotropies. As longitude and latitude always describe major parts of the variance of the climate variables, anisotropies have been modelled sufficiently by the regression step and only isotropic (or unsystematically varied) variogram structures are left in the residuals.

In the calculation of the exponential variograms, spherical distances of the stations were used (i.e. geographical coordinates were converted), otherwise large errors occur due to the size of East Asia. A unit lag of 50 km was used. Because the residuals are free of large-scale trends with respect to the effects of localized topography, global variograms were calculated. Naturally, the variograms of the residuals show less variability than the variograms of the climate variables.

Nevertheless, significant differences exist between variograms of individual years; in particular, precipitation follows different patterns throughout the year. The month of July is selected as an example for the monsoon season months; other months show similar variability. For instance, the years 1979 and 1980 exhibit contrasting patterns: in July 1979, precipitation occurred fairly evenly throughout the study area; in July 1980, large regional differences in precipitation were observed. Hence, in the variogram of 1980 (and similarly in 1981) the precipitation decreases more rapidly with distance than in the variogram of July 1979; the range is shorter in 1980 than in 1979 (Table II, Figure 6)

From a synoptic view, the model forms allow implications of dominant weather patterns, characterized by differences in homogeneity of air masses and resulting differences in precipitation types, such as mostly advective versus convective precipitation.

Months with precipitation patterns as in July 1979 are, in general, infrequent over 1951–90. The range as a characteristic distance describes the maximum distance over which (monthly) precipitation events are spatially correlated. This is a variable of considerable climatologic interest; the range is generally 1000–1200 km for that month of the year. There is a seasonal dependence, with a maximum during the late rainy season; at this time the interannual variability is also highest (Figure 7(a)).

Minimum values in January and the maximum in October are not typical, but depend on years with most unusual range values. However, the occurrence and frequency of years with unusual precipitation events may indicate a tendency for climatic change, as first indications of climatic change should occur in the form of a changed frequency of extreme events rather than in average conditions (Katz and Brown, 1992).

Variation of temperature residuals (Figure 8), exemplified again for July, exhibit a lower interannual variability and a lower spatial variability than precipitation variograms. The temperature has a large range (>2000 km), as temperature is a variable with spatial correlation over larger distances (Figure 7(b)). Interannual variability is about the same for each month of the year; this is also expected, because of the more constant spatial character of temperature.

Table II. Variogram parameters for precipitation in two years[a]

Date	Sill (mm^2)	Nugget (mm^2)	Range (km)	Model
July 1979	5×10^4	5.5×10^3	2500	Gaussian
July 1980	9.5×10^3	4×10^3	700	Linear

[a] Note the difference of range parameter in models!

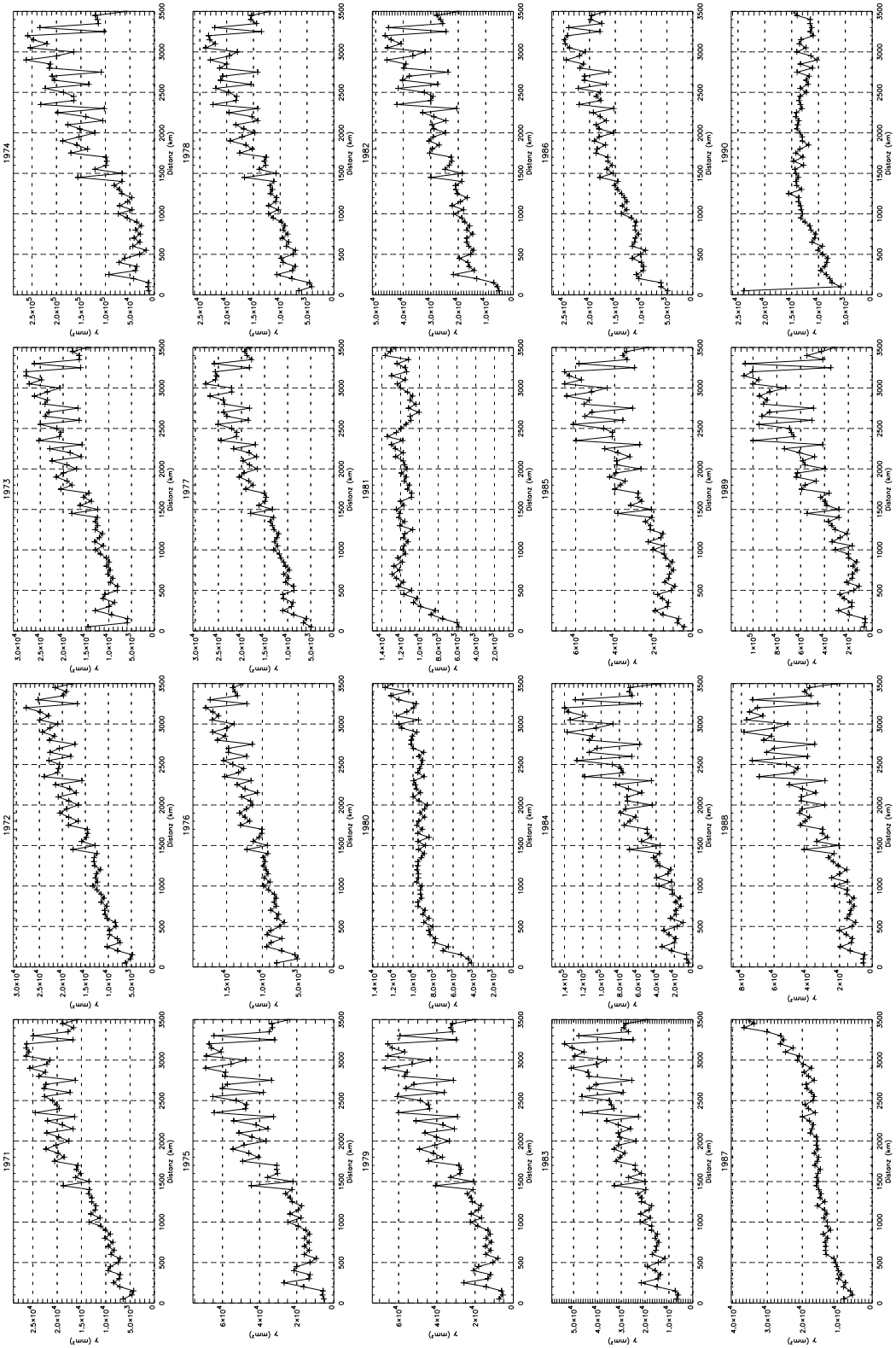

Figure 6. Variograms of monthly precipitation residuals for the month of July from 1971 to 1990

Variograms of PET residuals are given in Figure 9. They are noisy because observations were lacking at several stations prior to 1980, and because of problems in calculating PET. The range of PET (Figure 7(c)) is similar to that of precipitation, and the variograms show a decline of spatial correlation over relatively short distances — more similar to precipitation and in contrast to temperature. This is natural, as both PET and precipitation are directly, but inversely related to the occurrence of clouds. The seasonal dependency of the range parameter for PET, however, is similar to that of temperature, with high range values in summer. In a simplified look, the spatial variability of PET shares some characteristics with that of temperature owing to their joint dependence on seasonal sunshine variation and some characteristics with precipitation owing to their correlation with cloudiness influenced by small-scale topography.

5.1. Kriging and maps

In practice, a value for each raster element was obtained using the regression equation, then kriging was applied for every grid node to estimate the residual. Stations in areas outside of China were also included. Apart from geographical considerations, this eliminates edge effects for the area of China itself. In 8 of 480 cases, regression for PET data provided statistically insignificant results and had to be omitted. Instead, the maps for these months were calculated using geostatistics solely. An example of the regression result, kriging of residuals and of the final map is given in Figure 10.

Calculations were carried out on a personal computer (PIII 700 MHz). Because calculation of the residuals with 300″ resolution proved to be too time consuming on a personal computer, the final maps were calculated

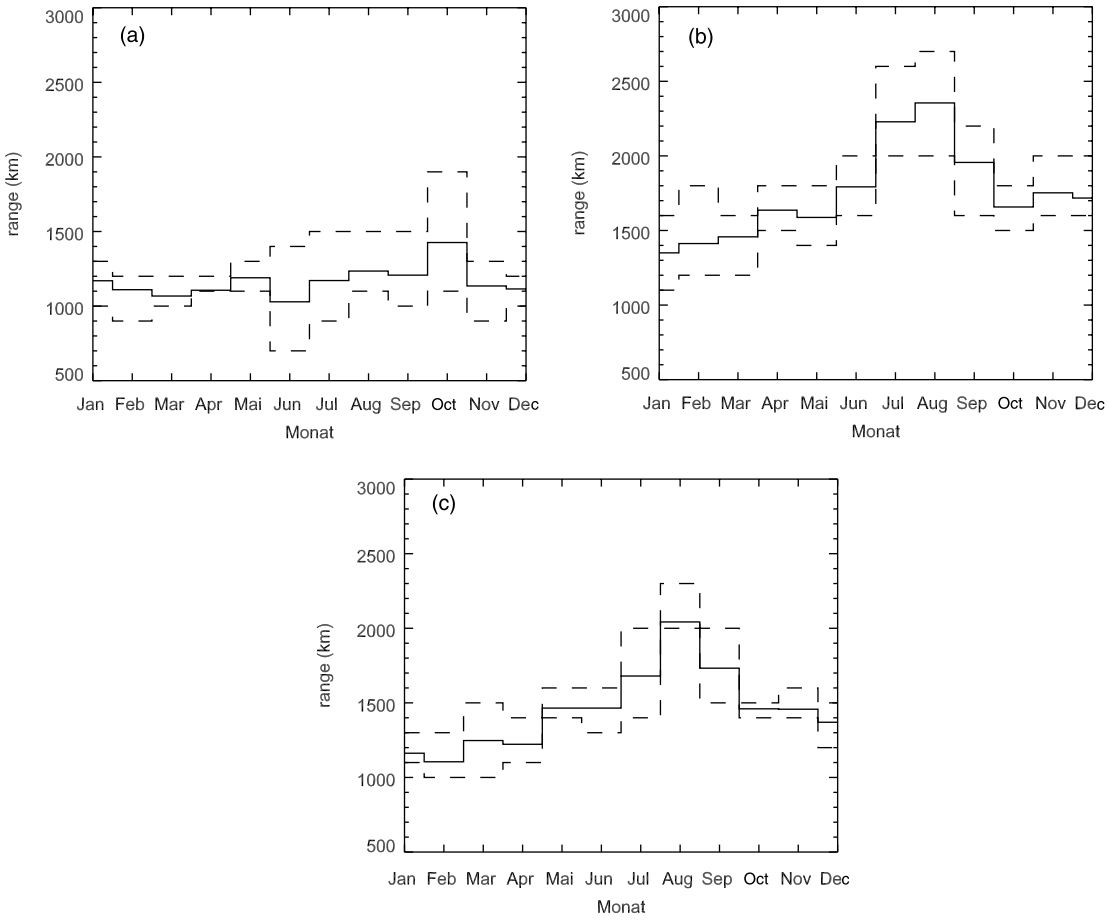

Figure 7. Seasonal variation of range of monthly (a) precipitation residuals, (b) temperature residuals, (c) PET residuals

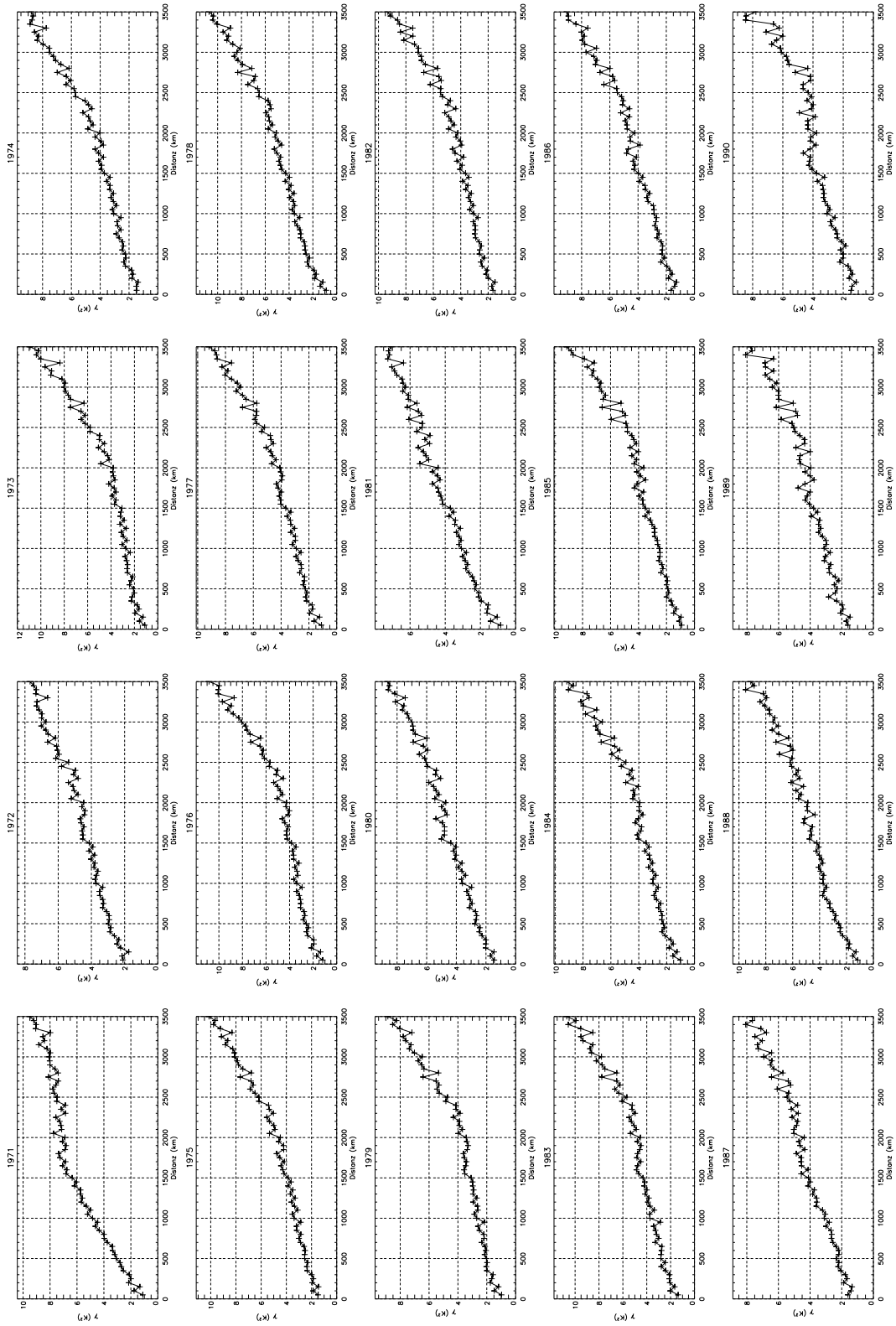

Figure 8. Variograms of monthly temperature residuals for the month of July from 1971 to 1990

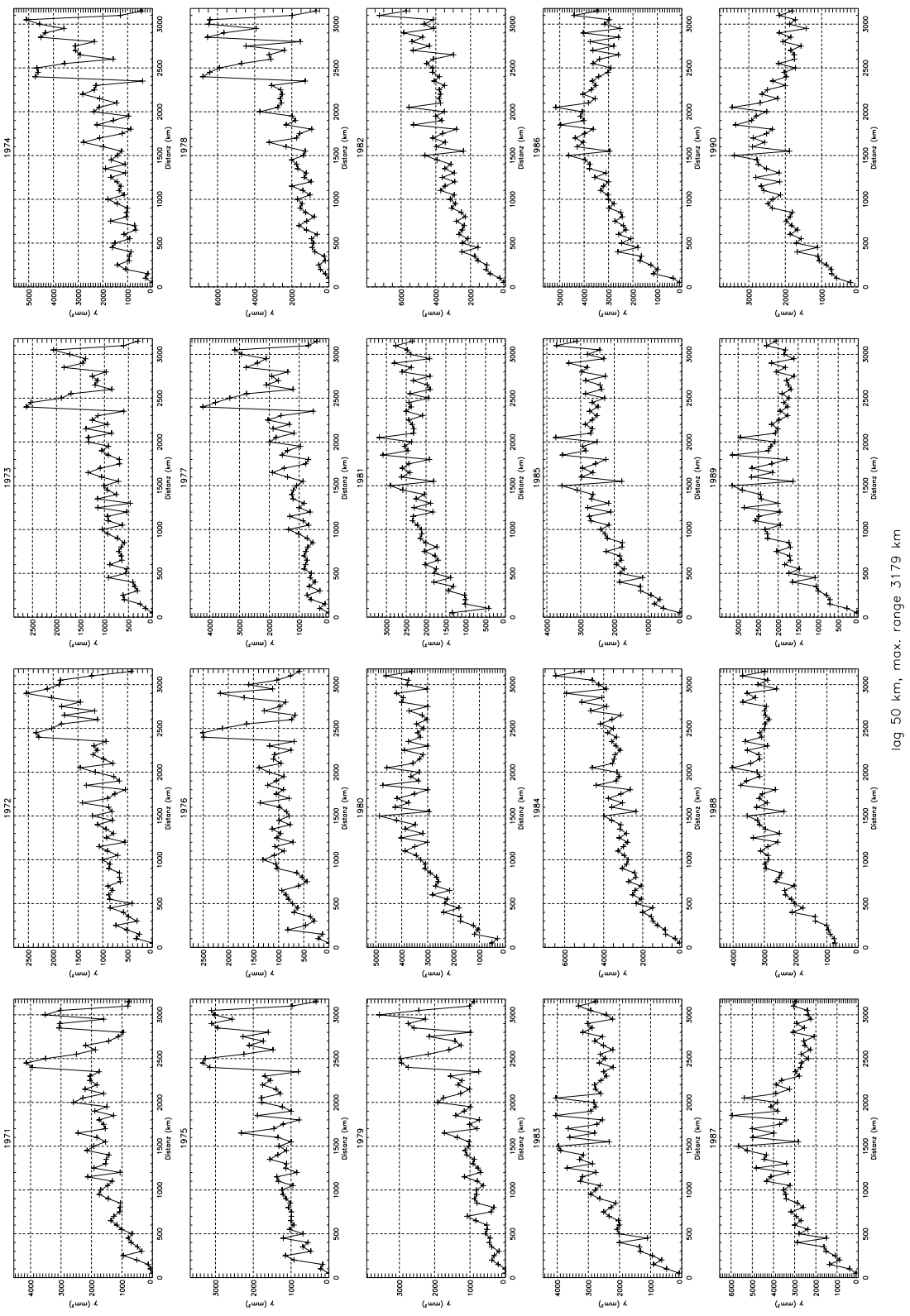

Figure 9. Variograms of monthly evapotranspiration residuals for the month of July from 1971 to 1990

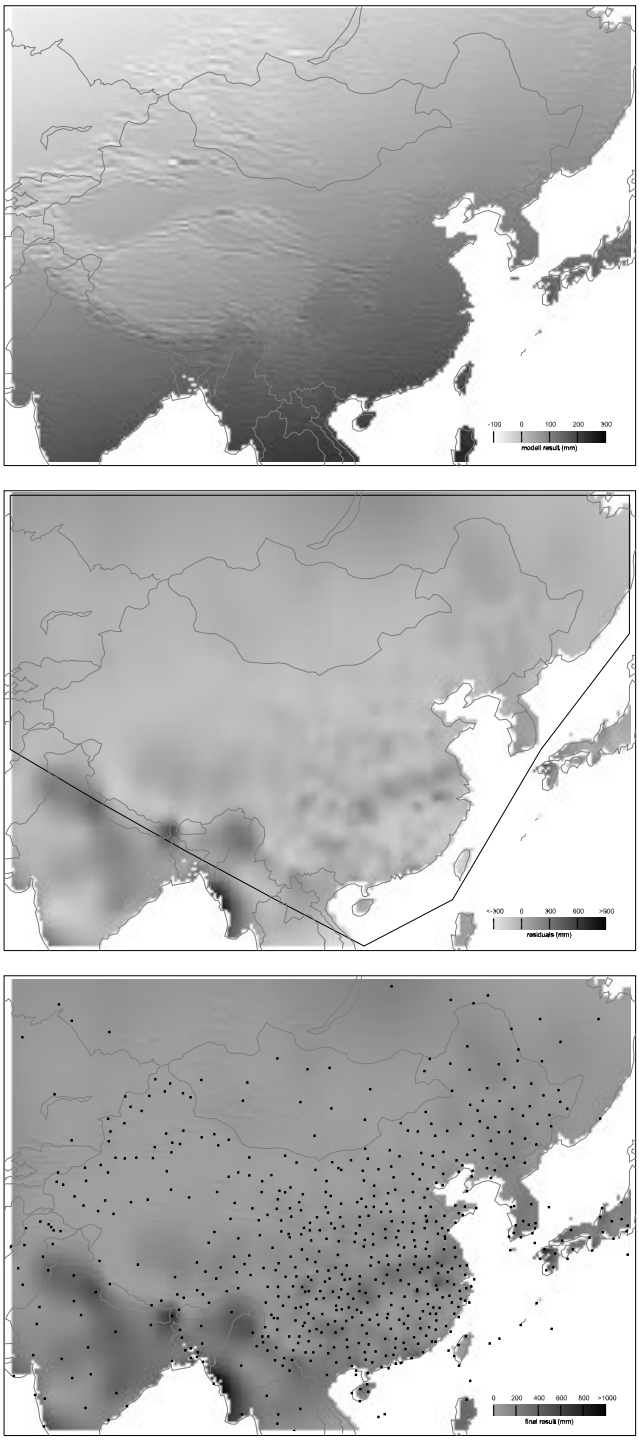

Figure 10. Results of regression analysis (top), kriging (middle) and final map (sum of regression and kriging, bottom) for July 1980 precipitation. Dots in the bottom map signify the stations available for this month. To enhance visibility of spatial differences within each map, precipitation is scaled individually for each map

for a resolution of $900'' = 0.25^{\circ}$; one map or monthly grid calculation took about 3.5 h. At this spatial resolution, morphological units such as large river valleys or intramontane basins that influence local climate and are important features for studies of regional ecosystems or hydrological research are still portrayed. In conclusion, the REGEOTOP method is sufficiently fast for computation of large models with higher resolution on a workstation.

6. RESULTS

It has been demonstrated that a PC-based parameterization of the topography of East Asia is able to explain more than 90% of variance of the input DEM data. The spatial arrangement of base topographies is consistent with a qualitative interpretation of the main topographic features of the East Asian continent. In case studies of contrasting mountain ranges (Massif Central, France; Black Forest, Germany; Tahiti islands, central Pacific), similar results were obtained by Benichou and Lebreton (1987), Klein (1994) and Wotling *et al*. (2000), who reported that about 70–90% of the original variance was retained in the first 10–15 PCs at DEM resolutions of 5 km, 250 m and 200 m respectively. Their base topographies closely resemble those obtained in this study, but arranged in a different order due to differences in the prevailing morphological features of East Asia, European interior mountain ranges, and isolated volcanic islands. PC-based topography parameterization appears to result in both statistically and physically sound results independent of DEM resolution and relief.

REGEOTOP was then applied to climate data from 12 months for 40 years (1951–90) for a total of 531, 672 and 196 stations (temperature, precipitation and PET respectively), which to our knowledge constitutes the most comprehensive climate time-series data collection available outside of China. After regression of the climate variables temperature, precipitation and PET with respect to base topographies and station location, residuals of the regression were analyzed in (a) variography and (b) kriging.

The results of the variography performed for the residuals of regression demonstrate that (a) spatial characteristics of each variable may be detected and (b) climatic characteristics may also be deduced. The spatial characteristics of precipitation residuals have a range of 1000–1200 km and a high spatial variability. Characteristics of temperature are a larger range of about 2500 km for most months and a high spatial correlation with low variability over much larger distances than observed for precipitation, as precipitation depends a lot more on local topographic forcing than temperature. With a range and spatial variability similar to that of precipitation, but a seasonal variation similar to that of temperature, PET may be considered as having an intermediate status between precipitation and temperature, as far as spatial variability is concerned. In addition to the spatial characteristics, climatological properties may be derived from the variography: seasonal variability is connected with the occurrence of the monsoons. Low or high variability indicates the prevalence of advective or convective precipitation events in respective years. It should be noted, however, that the modelling of the variograms in this paper is mostly done for mapping purposes and that a more detailed analysis of high-resolution structures may reveal more information on dependency on local relief (Herzfeld *et al*., 2003).

Owing to the large study domain, variables (latitude, longitude and altitude) describing the large-scale variability of the climatic elements contributed the major part of the explained variance. For temperature these three variables alone were sufficient to explain more than 80% of the variance throughout the year (Table II), confirming similar findings for the western Himalayas (Hormann, 1985). The contribution of exposure-related variables (PC_2 and PC_3) mostly remained low, as several air masses with different wind directions (e.g. southeast versus southwest monsoons) are active at the same time of year. In contrast, a number of complex topographic variables contribute to the explanation of the spatial organization of both precipitation (Figure 11) and PET (Figure 12). PC_7, PC_8 and PC_{12} are the most important topographic variables and represent base topographies that consist of systems of ridges, valleys and saddles (Figure 13). In particular, in mountains, the major part of topography-induced variability will be related to cloud formation and dissipation, which in turn is driven by surface flow structure and insolation differences over the dissected terrain. The above-mentioned PCs may represent topographic features that in some way strongly influence airflow, cloud distribution and, consequently, sunshine duration. However, it should be kept in mind that regressions are not able to detect physically

based mechanisms and that the observed relationship between topographic variables and observed climatic values may serve as a proxy for physical processes relating topographic forcing to precipitation and PET.

Mean explained variances of precipitation and PET (calculated as observed station value versus calculated grid value of the grid element containing the station) vary between 16 and 68% (Table III). Seasonal variation of explained variances points to the influence of different air mass characteristics that are mainly related to advective versus convective conditions. During both the summer and the winter monsoon seasons, advection occurs simultaneously over large areas and leads to climatically more homogeneous conditions that facilitate

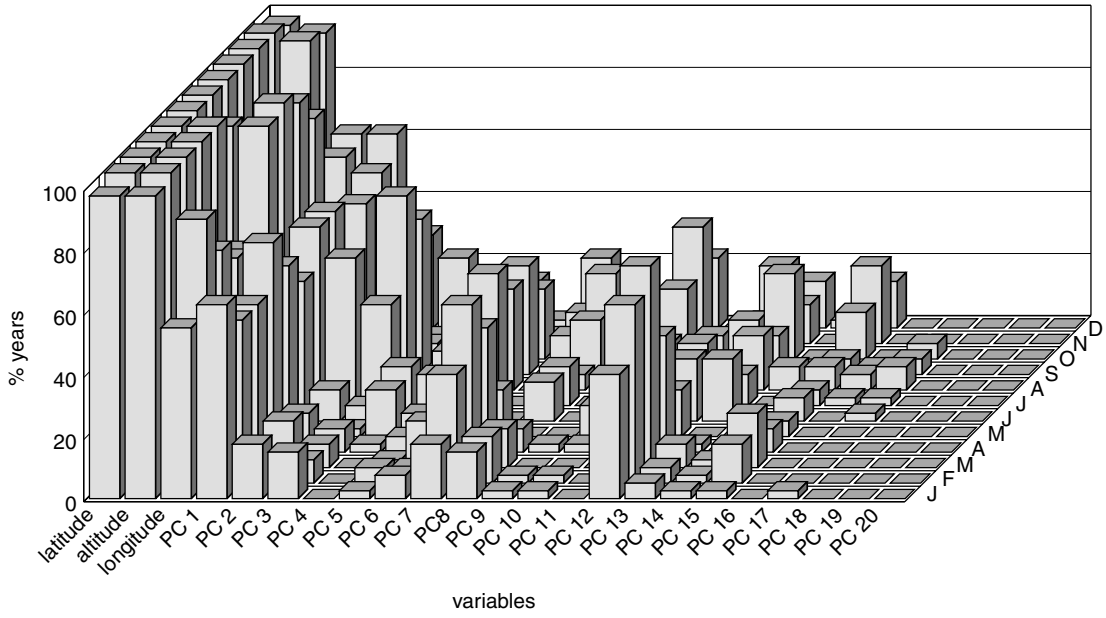

Figure 11. Relative frequency of contribution of independent variables to the regression equations for precipitation

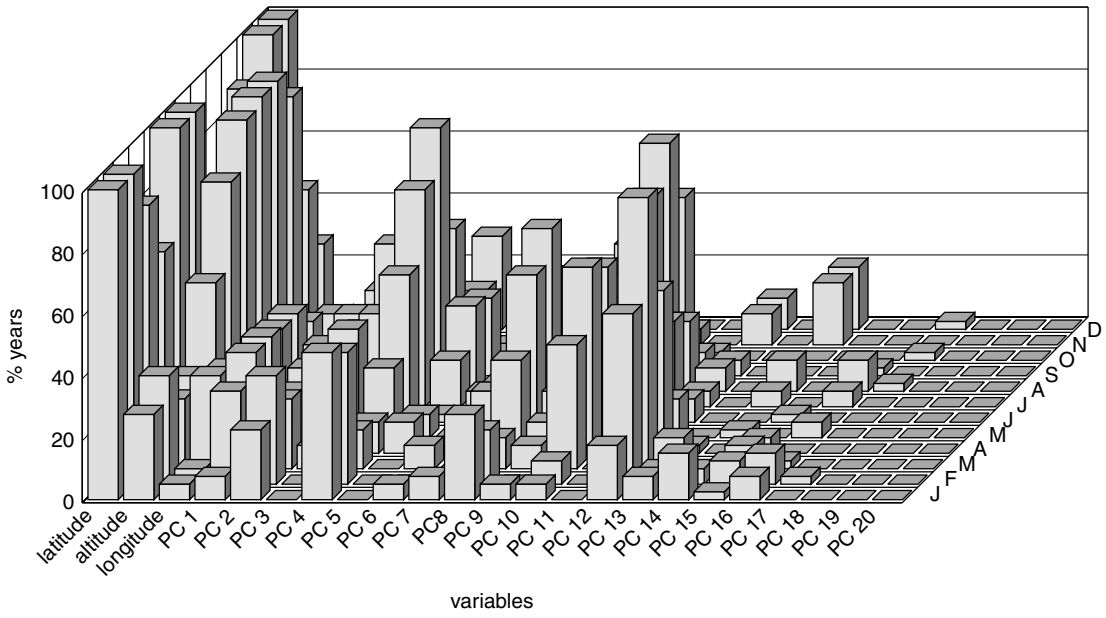

Figure 12. Relative frequency of contribution of independent variables to the regression equations for PET

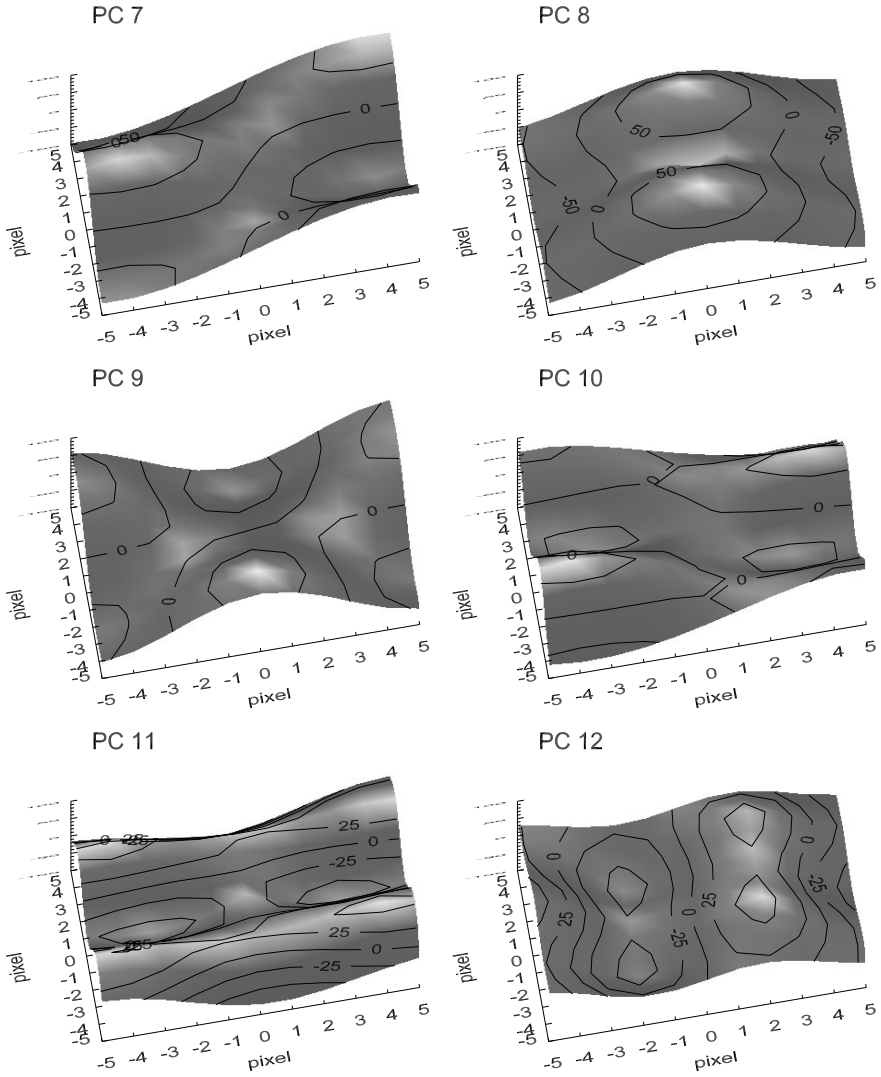

Figure 13. Spatial distributions of base topographies 7–12 in the study area. For a description see Figure 4

Table III. Minimum, maximum and average explained variances of temperature, precipitation and PET regression equations for the period 1951–90[a]

		Explained variance (%)											
		Jan	Feb	Mar	Apr	May	Jun	Jul	Aug	Sep	Oct	Nov	Dec
Temperature	Min.	89.5	89.7	87.6	82.9	80.2	71.2	77.1	82.9	85.1	93.2	90.8	91.4
	Max.	96.2	95.7	95.4	94.6	95.0	93.5	92.7	93.1	95.5	97.0	96.5	96.3
	Mean	94.1	93.4	91.8	89.0	88.0	87.6	87.5	89.2	93.5	95.2	94.5	94.1
Precipitation	Min.	9.1	10.6	16.6	20.8	18.4	8.7	2.8	6.5	8.0	6.2	7.7	2.1
	Max.	46.9	48.8	52.1	53.5	55.8	54.8	33.6	41.7	49.2	50.6	54.8	46.3
	Mean	27.7	31.1	32.5	36.0	38.2	29.7	15.8	23.2	26.7	27.5	28.6	23.7
PET	Min.	47.5	23.5	5.3	4.5	10.2	7.3	4.8	4.9	4.7	13.3	26.9	46.7
	Max.	83.1	80.4	38.9	40.8	57.6	57.6	48.2	53.9	52.7	58.4	74.4	83.0
	mean	65.1	48.9	21.5	15.4	30.7	32.2	24.7	25.7	29.9	37.2	54.3	67.4

easier spatial interpolation. The major part of the large differences between observed and calculated values have, however, to be attributed to the influence of the smoothed DEM data. With an average linear resolution of approximately 25 km, individual grid cells are not capable of resolving the actual topography: in the mountain regions of southwest China, the altitude range within a single grid cell may surpass 3000 m. This may be remedied by running REGEOTOP on a faster computer, using a smaller grid size. Consequently, grid-cell values should not even be expected to coincide closely with values observed at meteorological stations within the same grid cell (Fischer *et al*., 2000). In their smaller, climatically more homogeneous study regions, Benichou and Lebreton (1987) and Klein (1994) were able to capture at least 60% of the variance of monthly precipitation. Our tests, conducted in a small area of the southwest Chinese Mountains, indicate that up to 90% of the variance of monthly precipitation can be explained in months of homogeneous wind directions and strong topographic influence.

7. DISCUSSION

The results of this paper are relevant to several aspects of geoscience including:

1. An improved geomathematical method, i.e. REGEOTOP, a method that combines statistical and geostatistical principles (statistics and geostatistics).
2. Analysis of large data sets and cartographic representation (visualization and geographical information systems).
3. Production of new climate maps (climate research, ecosystem modelling, regional geography).

It should be noted that the method can barely be separated into a 'statistical part', 'data analysis part', 'geostatistical part' or 'geographic information systems part'; rather, it is one integrated approach oriented towards the solution of a geoscientific problem.

The parameterization of topography shown here can serve for a multitude of applications that need to address the influence of topography on spatial processes. An objective and reliable numerical representation of topography is particularly important in mountain research to investigate relief-induced effects on climate, vegetation distribution and snowmelt dynamics (Walsh *et al*., 1992). 'Base topographies' have been shown to describe topography with high precision at grid sizes from 200 m to 25 km, and should do so at any resolution. As conventional numeric raster data sets, 'base topographies' are easily integrated in a geographical information system and can be merged with any other spatial data set. They are particularly suitable for multivariate statistical analysis and allow easy classification of large areas with unsupervised or supervised classification procedures.

Although REGEOTOP can handle the regionalization of large areas, the results shown underline the need to analyse small, climatically homogeneous regions for optimum results. Even with the largest number of stations available in our data set, the station density is still not sufficient to analyse the climatic variability of the vast area in detail. For an estimation of spatial PET data of the contiguous USA, which are comparable in area and latitudinal extent to the People's Republic of China, Marks (1992) was able to use more than 1200 stations and still commented on data deficiency in several parts of the USA. A less restrictive data distribution policy by the Chinese authorities for the vast pool of climatic data of at least 2000 stations available in the People's Republic of China would allow a far more thorough analysis.

Despite these shortcomings, a comparison of our maps with previously published hand-drawn maps (Domrös and Peng, 1986; Zhang and Lin, 1992; Feng, 1993) allows one to appreciate the superiority of the new maps, both due to the increased data volume and to the mathematical and computer-based mapping methods. In general, large-scale features are virtually identical. Maps derived from topography-based regionalization procedures can, however, display reliable information for regions where no climatic data are available due to lack of meteorological stations. This effect is particularly visible in mountainous areas, where regional detail is far more pronounced than in the hand-drawn maps. As an example, the effects of small-scale topographic features are easily visible, such as the distinctive precipitation areas induced by orographic lifting along the

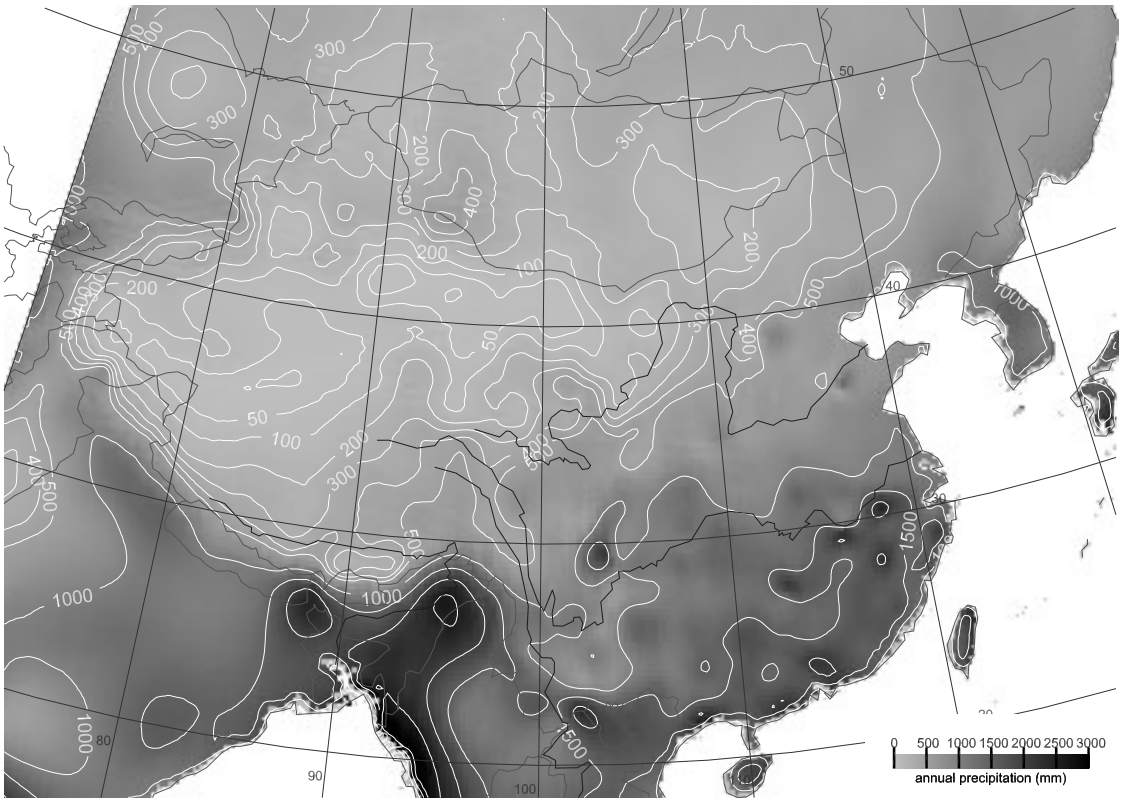

Figure 14. Map of mean annual precipitation (1951–90) averaged from monthly precipitation data fields. Isohyets added for clarity are based on low-pass-filtered data and are approximate

small Dabashan Mts (*ca.* 23 °N, 107 °E), a region of maximum precipitation in mainland China, and windward and leeward (rain shadow) effects on the east and west slopes respectively of the Taiwan Mts, Taiwan. (Figure 14). Some examples of the maps are available at http://www.geo.uni-mainz.de/thomas/regeotop.

Compared with other climatic data sets that cover East Asia (Leemans and Cramer, 1991; New *et al*., 1999, 2002) or China (Baker, 1999; Prieler, 1999), these data offer high-resolution time series that reflect topography-induced variability to a much higher degree. Compared with the 'PRISM' data computed by Daly *et al*. (2000), who only utilized monthly means and did not include PET, our maps have the advantage of including monthly spatial time series, and thus enable the study of both seasonal and decadal variability. In addition, the data set presented here is the only high-resolution data that contains Penman–Monteith evapotranspiration estimates for China. Extending the database until 2000, increasing station density, particularly in mountain areas, and increasing output resolution will result in further improvements in the future. The maps presented here provide a data basis that is suitable for verification of global climate models, for hydrological studies and for agro-ecological investigations and prognoses for East Asia.

ACKNOWLEDGEMENTS

Support by Deutsche Forschungsgemeinschaft fellowship TH/635-2 to A.T. is gratefully acknowledged. U.C.H. would like to thank the Cooperative Institute for Research in Environmental Sciences, University of Colorado Boulder, for a CIRES Visitor Fellowship.

APPENDIX: REGEOTOP ALGORITHM

Do Step (1) once for the DEM

1. Determination of basis relief types using PCA, applied to 11×11 grid moving windows and $N \times M$ grid locations (where $N \times M$ is size of DEM raster) $\rightarrow k$ principal components (here $k \approx 16$).

Do Step (2) to Step (6) $\alpha \times \beta \times \gamma$ times (here $3 \times 12 \times 40 = 1440$ times)

2. Regression analysis of climate variables $V_{\alpha,\beta,\gamma}$ using coordinates x, y, z (longitude, latitude, and elevation) and the PCs $PC_1, \ldots, PC_k$ as independent variables and $V_{\alpha,\beta,\gamma}$ as dependent variable (for each α, β, γ; here: α variable type: temperature, precipitation, PET; $\beta = 1, \ldots, 12$ months; $\gamma = 1950, \ldots, 1990$, year).
3. Calculate residuals of (2) (for each α, β, γ).
4. Variography of residuals $\varepsilon_{\alpha,\beta,\gamma}(x, y)$ in $\mathcal{R}^2$ (for each α, β, γ).
5. Kriging (ordinary kriging) of residuals $\varepsilon_{\alpha,\beta,\gamma}(x, y)$ in $\mathcal{R}^2$ (for each α, β, γ) and mapping of residuals (for each α, β, γ).
6. Add up regression estimates and kriged residuals to obtain a final map (for each α, β, γ).

REFERENCES

Ahmed S, De Marsily G. 1987. Comparison of geostatistical methods for estimating transmission data on transmitivity and specific capacity. *Water Resources Research* **23**: 1717–1737.

Allen RG, Pereira LS, Raes D, Smith M. 1998. Crop evapotranspiration. *FAO Irrigation and Drainage Paper* 56.

Baker CB. 1999. Area averaged temperature time series for China, India and the United States. http://lwf.ncdc.noaa.gov/oa/climate/online/doe/doe.html [13 February 2002].

Basist A, Bell GD, Meentemeyer V. 1994. Statistical relationships between topography and precipitation patterns. *Journal of Climate* **7**: 1305–1315.

Benichou P, Lebreton O. 1987. Prise en compte de la topographie pour la cartographie des champs pluviométriques statistiques. *Météorologie 7. Série*, no. 19.

Böhner J. 1996. Säkuläre Klimaschwankungen und rezente Klimatrends Zentral- und Hochasiens. Göttinger Geographische Abhandlungen, 101.

Buishand TA. 1982. The analysis of homogenity of long-term rainfall records in the Netherlands. Koninklijk Nederlands Meteorologisch Instituut Scientific Report, 86–7.

Chilès J-P, Delfiner P. 1999. *Geostatistics. Modeling Spatial Uncertainty*. Wiley: New York.

Daly C, Taylor GH, Gibson WP. 1997. The PRISM approach to mapping precipitation and temperature. In *10th AMS Conference on Applied Climatology*, American Meteorological Society: Boston; 10–12.

Daly C, Gibson WP, Hannaway D, Taylor GH. 2000. Development of new climate and plant adaptation maps for China. In *12th AMS Conference on Applied Climatology*, American Meteorological Society: Boston; 62–65.

Domrös M, Peng G. 1986. *The Climate of China*. Springer: Berlin.

Feng X. 1993. Introduction to climate and agriculture in China. In *Climate and Agriculture in China*, Cheng C (ed.). China Meteorological Press: Beijing; 1–29.

Fischer G, van Velthuizen H, Nachtergaele FO. 2000. Global agro-ecological zones assessment: methodology and results. IIASA Technical Report IR-00–064. International Institute for Applied Systems Analysis, Laxenburg, Austria.

Fleming MD, Chapin FS, Cramer WP, Hufford GL, Serreze MC. 2000. Geographic patterns and dynamics of Alaskan climate interpolated from a sparse station record. *Global Change Biology* **6**: 49–58.

Fliri F. 1967. Über die klimatologische Bedeutung der Kondensationshöhe im Gebirge. *Die Erde* **98**: 203–210.

Goovaerts P. 2000. Geostatistical approaches for incorporating elevation into the spatial interpolation of rainfall. *Journal of Hydrology* **228**: 113–129.

Hay L, Viger R, McCabe G. 1998. Precipitation interpolation in mountainous regions using multiple linear regressions. In *Hydrology, Water Resources and Ecology in Headwaters*, Kovar K, Tappeiner U, Peters NE, Craig RG (eds). IAHS Publication No. 248. IAHS Press: Wallingford; 33–38.

Herzfeld UC. 1990. Geostatistical software for evaluation of line survey data applied to radio-echo sounding in glaciology. In *Microcomputer Applications in Geology II*, Hanley JT, Merriam DF (eds). Pergamon Press: Oxford; 119–136.

Herzfeld UC. 1992. Least squares collocation, geophysical inverse theory, and geostatistics: a bird's eye view. *Geophysical Journal International* **111**: 237–249.

Herzfeld UC, Mayer H, Caine N, Losleben M, Erbrecht T. 2003. Morphogenesis of typical winter and summer snow surface patterns in a continental alpine environment. *Hydrological Processes* **17**: 619–649.

Hess T, Stephens W. 1993. The Penman equation. In *Spreadsheets in Agriculture*, Noble DH, Courte CP (eds). Longman: London; 184–194.

Holdaway MR. 1996. Spatial modelling and interpolation of monthly temperature using kriging. *Climate Research* **6**: 215–225.

Hormann K. 1985. Niederschlagsverteilung in den westlichen Himalaya-Ländern. In *Internationales Symposium über Tibet und Hochasien*, 8–11 October, Göttingen, Germany, Kuhle M (ed.). Göttinger Geographische Abhandlungen, 81; 241–255.

Hudson G, Wackernagel H. 1994. Mapping temperature using kriging with external drift: theory and an example from Scotland. *International Journal of Climatology* **14**: 77–91.

Hughes DA. 1982. The relationship between annual rainfall and physiographic variables applied to a coastal region of southern Africa. *South African Geographical Journal* **64**: 41–50.

Hutchinson MF. 1995a. Interpolating mean rainfall using thin plate smoothing splines. *International Journal of Geographical Information Systems* **9**: 385–403.

Hutchinson MF. 1995b. A new objective method for spatial interpolation of meteorological variables from irregular networks applied to the estimation of monthly mean solar radiation, temperature, precipitation and windrun. CSIRO Division of Water Resources Technical Memo 89/5; 95–104.

Kaiser D, Tao S, Fu C, Zeng Z, Zhang Q, Wang W, Karl T. 1993. Climate data bases of the People's Republic of China, 1841–1988. US Department of Energy Technical Report 55, DOE, Washington.

Katz RW, Brown BG. 1992. Extreme events in a changing climate: variability is more important than averages. *Climate Change* **21**: 289–302.

Klein G. 1994. Regionalisierung von Niederschlag mit Hilfe digitaler Geländeinformationen. Freiburger Geographische Hefte 44.

Konrad C. 1996. Relationships between precipitation event types and topography in the southern Blue Ridge mountains of the southeastern USA. *International Journal of Climatology* **16**: 49–62.

Leblois E, Desurosne I. 1994. Regionalisation of rain intensities on the French Alpine area: a methodological test for interpolation in mountainous areas. In *Proceedings, Development in Hydrology in Mountainous Areas*, 12–16 September, Stará Lesná, Slovakia; 60–69.

Leemans R, Cramer WP. 1991. The IIASA database for mean monthly values of temperature, precipitation, and cloudiness on a global terrestrial grid. IIASA Report RR-91–018. International Institute for Applied Systems Analysis, Laxenburg, Austria.

Marks D. 1992. A continental-scale simulation of potential evapotranspiration for historical and projected doubled-CO_2 climate conditions. Environmental Protection Agency EPA/600/3-90/078. EPA, Corvallis. http://www.ngdc.noaa.gov/seg/eco/cdroms/gedii_b/datasets/b12/ec.htm [10 July 2002].

Martinez-Cob A. 1996. Multivariate geostatistical analysis of evapotranspiration and precipitation in mountainous terrain. *Journal of Hydrology* **174**: 19–35.

Mitchell JM. 1966. Climatic change. World Meteorological Organisation Technical Note, 79.

New MG, Hulme M, Jones PD. 1999. Representing 20th century space–time climate variability. I: development of a 1961–1990 mean monthly terrestrial climatology. *Journal of Climate* **12**: 829–856.

New MG, Lister D, Hulme M, Makin I. 2002. A high-resolution data set of surface climate over global land areas. *Climate Research* **21**: 1–25.

Parker AJ. 1982. The topographic relative moisture index: an approach to soil moisture assessment in mountainous terrain. *Physical Geography* **3**: 160–168.

Peck EL, Brown MJ. 1962. An approach to the development of isohyetal maps for mountainous areas. *Geophysical Research* **67**: 681–694.

Peterson TC, Vose RS. 1997. An overview of the Global Historical Climatology Network temperature data base. *Bulletin of the American Meteorological Society* **78**: 2837–2849.

Phillips DL, Dolph J, Marks D. 1992. A comparison of geostatistical procedures for spatial analysis of precipitation in mountainous terrain. *Agricultural and Forest Meteorology* **58**: 119–141.

Prieler S. 1999. Temperature and precipitation variability in China — a gridded monthly time series from 1958–1988. IIASA Interim Report IR-99–074. International Institute for Applied Systems Analysis, Laxenburg, Austria.

Prudhomme C, Reed DW. 1998. Relationships between daily precipitation and topography in a mountainous region: a case study in Scotland. *International Journal of Climatology* **18**: 1439–1453.

Prudhomme C, Reed DW. 1999. Mapping extreme rainfall in a mountainous region using geostatistical techniques: a case study in Scotland. *International Journal of Climatology* **19**: 1337–1356.

Ren M. 1985. *An Outline of China's Physical Geography*. Foreign Languages Press: Beijing.

Richman MB. 1986. Rotation of principal components. *Journal of Climate* **5**: 379–388.

Scherer JC. 1977. Une méthode d'extrapolation dans l'espace de données pluviométriques moyennes. Application à une partie des Vosges et à leur bordure. *Recherches Gèographiques* **4**: 69–85.

Schermerhorn VP. 1967. Relations between topography and annual precipitation in western Oregon and Washington. *Water Resources Research* **3**: 707–711.

Schönwiese C-D, Malcher J. 1985. Nicht-Stationarität oder Inhomogenität? Ein Beitrag zur statistischen Analyse klimatologischer Zeitreihen. *Wetter und Leben* **37**: 181–193.

Spreen WC. 1947. Determination of the effect of topography on precipitation. *Transactions of the American Geophysical Union* **28**: 285–290.

Tao S, Fu C, Zeng Z, Zhang Q. 1991. Two long-term instrumental climatic data bases of the People's Republic of China. ORNL/CDIAC-47, NDP-039. Carbon Dioxide Information Analysis Center, Oak Ridge National Laboratory, Tennessee. (Additions: 1997.) http://cdiac.esd.ornl.gov/ndp039.htm [12 August 1999].

Thomas A. 1997. The climate of the Gongga Shan Range, Sichuan Province, PR China. *Arctic and Alpine Research* **29**: 226–232.

USGS. 2000. GTOPO30. http://edcwww.cr.usgs.gov/landdaac/gtopo30 [15 November 2000].

Walsh SJ, Butler DR, Brown DG, Bian L. 1992. Form and pattern in the alpine environment: an integrated approach to spatial analysis and modelling in Glacier National Park, USA. In *GIS and Mountain Environments*, Price MF, Heywood DI (eds). Taylor and Francis: London; 189–216.

WMO. 1972. Distribution of precipitation in mountainous areas. Geilo-Symposium, July 31–August 5, Norway. WMO Technical Note, 326.
Wotling G, Bouvier C, Danloux J, Fritsch J-M. 2000. Regionalization of extreme precipitation distribution using the principal components of the topographical environment. *Journal of Hydrology* **233**: 86–101.
Zhang J, Lin Z. 1992. *The Climate of China*. Wiley: New York.

